

Natural convection in air-filled horizontal cylindrical annuli

D. Alshahrani and O. Zeitoun

Mech. Eng. Dept., College of Engineering, King Saudi University, Riyadh, Saudi Arabia

Natural convection in horizontal cylindrical annuli was investigated numerically using finite element technique together with SIMPLER algorithm. Annulus geometric configurations of $D_o/D_i = 2, 3, 4$ and 5 were investigated. Laminar conditions up to Rayleigh number Ra_i of 10^5 were investigated. Flow fields represented by stream lines, velocity vectors and isothermal lines were presented for various conditions. The data of heat transfer, represented by Nusselt number Nu_i and effective thermal conductivity ratio k_e/k were presented versus Rayleigh number Ra_i . The data of effective thermal conductivity ratio k_e/k were presented versus a new modified Rayleigh number Ra_m . Three regimes of heat transfer were observed; conduction dominated, transition and convection dominated regimes. The data of heat transfer, represented by the effective thermal conductivity ratio k_e/k were correlated and comparison with existed experimental data indicates the accuracy of new correlations.

تم دراسة انتقال الحرارة بالحمل الحراري الطبقي الطبيعي في الفجوة بين اسطوانتين افقيتين متحدتي المحور عدديا باستخدام طريقة العناصر المحددة لنسب اقطار 2 و 3 و 4 و 5. وقد عرضت النتائج على شكل كونتورات لدالة السريان ودرجات الحرارة و توزيعات لدرجات الحرارة و السرعات و الفيض الحراري. تم الحصول على نتائج لانتقال الحرارة في شكل رقم نسلت و النسبة بين معامل التوصيل الحراري المكافئ الى معامل التوصيل الحراري مع رقم رايلي لنسب اقطار مختلفة. تم استنتاج رقم رايلي معدل لتجميع النتائج في علاقة وحيدة وقد قورنت هذه العلاقة مع بعض النتائج العملية المتوفرة لهذا النوع من السريان حيث بينت المقارنات التوافق الجيد للعلاقة المقترحة و هذه النتائج.

Keywords: Natural convection, Heat transfer, Laminar, Horizontal, Cylindrical annuli

1. Introduction

Natural convection in horizontal annulus has been widely investigated due to its practical relevance to many engineering applications including microelectronic systems, solar concentrators, thermal storage plants, pressurized water reactors and gas insulated electrical transmission systems [1-16]. Detailed review of natural convection heat transfer in horizontal annuli was presented by Teertstra and Yovanovich [17].

Liu et al. [1] conducted an experimental investigation of horizontal annuli for different aspect ratios and fluids and proposed a correlation for effective thermal conductivity ratio.

Grigull and Hauf [2] used thermal interferometry to visualize the temperature and flow fields in air-filled horizontal circular annuli. Their visual observation indicated that the flow patterns took the kidney shape and as Grashof number increased the centers of the closed flow circulation moved up. Grigull

and Hauf [2] identified three distinct natural convection regimes in the horizontal annuli: the pseudo-conductive region ($Gr_\delta < 2400$) where the heat transfer is independent of Gr_δ , the transition region ($2400 \leq Gr_\delta \leq 30000$), and the fully developed convective region ($Gr_\delta > 30000$) where the convection mechanism is the dominant. Visualizations of [2] show that the isotherms are slightly eccentric around the inner tube in the first regime where the conduction mechanism is the dominant in this regime. In the second regime, the isotherms are still eccentric but slightly deformed towards the upper parts of the outer cylinder. In the third regime, the isotherms form a mushroom shape along the upper part of the outer cylinder.

Lis [3] carried out an experimental study for natural convection in air-filled horizontal simple circular annuli or containing helical and axial spacers. The six axial spacers used in the obstructed annuli enhanced heat transfer effects (compared to the simple an-

nuli) due to more efficient mixing near the upper parts of the annulus.

Bishop et al. [4] visualized the natural convection flow in annuli. They observed two basic types of flow; the crescent and the kidney-shaped eddy patterns. In both patterns, the fluid flows up along the inner cylinder surface at a relatively high velocity when compared to the velocity of the fluid in the central and major portion of the eddy. The primary differences between these two patterns are the shape of the central low speed region and the size of the nearly stagnant region in the lower portion of the annulus. For a relative gap width of 1.35 and a Grashof number based on inner cylinder diameter of 1.5×10^5 , they observed that the normally stable kidney-shaped eddy pattern became unstable and began to oscillate tangentially.

Itoh et al. [5] proposed a new method for correlating heat transfer coefficients for natural convection in horizontal cylindrical annuli. The characteristic length was chosen as the geometric mean of the inner and outer cylinder radii combined with the conduction shape factor for the annulus.

Kuehn and Goldstein [6] carried out experimental and numerical investigations for natural convection flow in horizontal annuli for Rayleigh number in the range 2.11×10^4 to 9.76×10^5 . According to their observations, the flow and heat transfer results can be divided into several regimes. Below Rayleigh number of 100, the center of rotation is near 90° . A transition region exists for Rayleigh number between 10^2 and 3×10^4 . The flow remains of the same pattern but becomes strong enough to influence the temperature field. Steady laminar boundary layer regime exists between Rayleigh numbers of 3×10^4 and 10^5 . For air, the flow starts to have oscillation near Rayleigh numbers of 10^5 . Kuehn and Goldstein [7] proposed a correlation for Nusselt number based on Nusselt numbers in first and third regimes.

Raithby and Hollands [8] introduced a model based on two conduction layers adjacent to the inner and outer surfaces of the annulus. The model divides the laminar natural convection in annulus into two domains; the conduction dominated regime where $k_e/k = 1$ and

the convection dominated domain where $k_e/k > 1$.

Kumar [9] investigated numerically the natural convection in horizontal annuli for Rayleigh number from 100 to 10^7 for diameter ratios from 1.2 to 10 under uniform wall heat flux condition at the surface of the inner cylinder while outer cylinder was kept at isothermal conditions. He concluded that the flow pattern was affected by the diameter ratio of the annulus and the Rayleigh number.

Yoo [10] observed instability in narrow annuli at low Prandtl number. For Prandtl number, $Pr \leq 0.2$, the flow has steady or oscillatory flows consisting of multiple like-rotating cells. For $Pr = 0.3$, the flow has one counter-rotating cell on the top of the annulus. Yoo [11] investigated the existence of dual solutions in natural convection in horizontal annulus for the fluids of $0.3 \leq Pr \leq 1$. Two kinds of flow patterns are realized: the first is the crescent shaped eddy pattern in which the fluid in the top of the annulus ascends. In the second, the fluid descends by forming two counter rotating eddies in a half annulus.

Crawford and Lemlich [12] studied natural convection of air between horizontal cylindrical annuli. They numerically examined three different radius ratios, $R = 2, 8$ and 57 , and confined their study to extremely low Grashof number, the so called creeping flow solution. Their results revealed the characteristic kidney shaped circulation pattern.

Farouk and Guceri [13] studied numerically natural convection in annulus for laminar and turbulent flow. They found that below a Rayleigh number of 10^2 the velocities are too small to affect the temperature distribution, which remains essentially as in pure conduction. A transition region exists for Rayleigh number between 10^2 and 3×10^4 . All of their test cases pertained to $R = 2.6$ with vertical symmetry assumed.

Kolesnikov and Bubnovich [14] investigated conjugate unsteady state natural convection in horizontal annuli. They reported that the conduction inside walls of channels greatly affects the natural convection heat transfer in the annuli.

Kim and Ro [15] solved the steady-state two-dimensional natural convective heat transfer in horizontal cylindrical annuli. Two

families of convergent solutions were found for moderate values of outer-to-inner radius ratio and high Rayleigh numbers, depending on the initial guesses for the field variables. Particularly for a narrow annulus, tricellular solutions also were observed to exist, and only the multicellular solutions were viable as the Rayleigh number exceeded a certain critical value. It was also found that the numerical determination of the bifurcation points required very restrictive criteria for convergence.

Elsherbiny and Moussa [16] investigated numerically the natural convection in horizontal annuli for Rayleigh number from 100 to 10^6 for diameter ratios from 1.25 to 10. They concluded that the annular gap can represent a single inner cylinder in an infinite medium for annulus diameter ratio of 10 for Rayleigh number $\leq 10^5$. They also proposed a correlation based on the modification of correlation of [6 and 7].

In this paper, steady state laminar natural convection heat transfer in a horizontal cylindrical annulus was investigated numerically. A numerical study was conducted to obtain the velocity and temperature distributions within the annulus and the heat transfer between the two surfaces of the annulus. The effect of geometric parameters on the flow and heat transfer between the two surfaces was investigated.

2. Analysis

The physical description of the investigated problem is illustrated schematically in fig. 1. A hot surface cylinder of diameter D_i is placed inside another cylinder of diameter D_o trapping air in the resulting annular cavity. The inner cylinder is placed concentric with the outer cylinder as shown in fig. 1. As the inner cylinder is hotter than the outer one, a buoyancy induced flow results and natural convection occurs. The surface of the inner and outer cylinders are assumed to be isothermal at T_i and T_o , respectively, where $T_i > T_o$. The enclosure was assumed very long. Consequently, the flow in the gap was considered a two-dimensional flow of horizontal coordinate x and vertical coordinate y . The

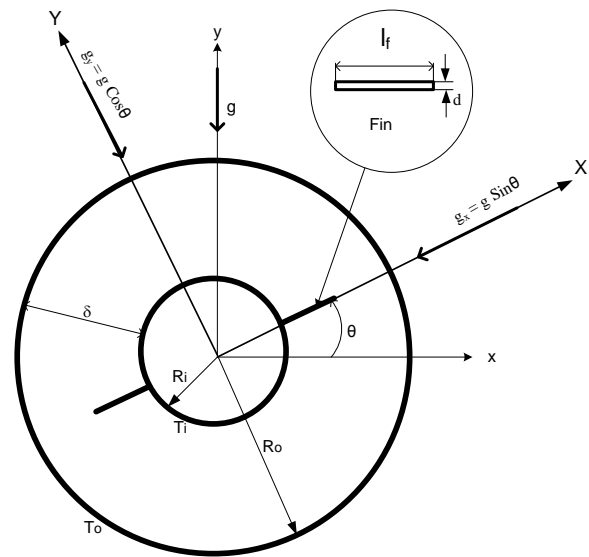


Fig. 1. Physical description and coordinate system of the current problem.

flow is assumed to be steady and laminar and the fluid is Newtonian. The viscous dissipation within the fluid is assumed to be negligible.

The partial differential equations governing the fluid flow and heat transfer in the enclosure include the continuity, momentum, and energy equations. For the above assumptions, the continuity equation is:

$$\frac{\partial u}{\partial x} + \frac{\partial v}{\partial y} = 0 \quad \frac{\partial u}{\partial x} + \frac{\partial v}{\partial y} = 0. \quad (1)$$

The momentum equations in x and y directions are:

$$\rho u \frac{\partial u}{\partial x} + \rho v \frac{\partial u}{\partial y} = -\frac{\partial P}{\partial x} + \mu \left[\frac{\partial^2 u}{\partial x^2} + \frac{\partial^2 u}{\partial y^2} \right], \quad (2)$$

$$\rho u \frac{\partial v}{\partial x} + \rho v \frac{\partial v}{\partial y} = -\rho g - \frac{\partial P}{\partial y} + \mu \left[\frac{\partial^2 v}{\partial x^2} + \frac{\partial^2 v}{\partial y^2} \right]. \quad (3)$$

Where g is the gravitational acceleration in y direction. The energy equation is:

$$\rho C_p u \frac{\partial T}{\partial x} + \rho C_p v \frac{\partial T}{\partial y} = k \left[\frac{\partial^2 T}{\partial x^2} + \frac{\partial^2 T}{\partial y^2} \right]. \quad (4)$$

For natural convection flow, the change in density is responsible for the flow and the ideal gas equation of state was provided as an input to estimate the fluid density,

$$\rho = \frac{P}{RT}, \quad (5)$$

where P is the absolute pressure. The reference pressure was assumed equal to the standard atmospheric pressure during the current investigation. The properties of air except density are assumed constant and are taken to be the values at the mean temperature,

$$T_m = \frac{T_i + T_o}{2}. \quad (6)$$

The governing eqs. (1-5) must satisfy the following boundary conditions:

1. At outer surface ($R = R_o$); $T = T_o$ & $u = v = 0$
2. At inner surface ($R = R_i$); $T = T_i$ & $u = v = 0$

3. Solution procedure

The governing eqs. (1) - (4) are solved numerically using Cosmos-Flow Plus software which was derived from the SIMPLER solution scheme introduced by Patankar [18]. This software was recently used by Zeitoun [19] to study the heat transfer and flow fields by natural convection from a vertical plate enclosed in a horizontal cylinder, and Zeitoun and Ali [20] to study natural convection around horizontal rectangular ducts. This code uses the finite element method to obtain approximate solutions of the original partial differential equations. By using this method, the governing partial differential equations are reduced to a set of algebraic equations. The dependent variables are represented by polynomial shape functions over a small area or volume (element). These representations are substituted into the governing equations and then the weighted integral of these equations over the element is taken where the weight function is chosen to be the same as the shape function. The result is a set of algebraic equations for the dependent variable at discrete points or nodes on every element. By assuming a simple form of solution in each

finite element, the approximate solution of the problem in the complete domain is determined. The pressure-velocity coupling is solved by using the well known SIMPLER method [18] where the pressure is first solved using assumed velocity components. Velocity correction equations are then solved to correct velocities. The pressure and velocity fields are then corrected based on calculated values of pressure and velocities. This process is repeated until the residual of all equations are negligible.

A four node quadrilateral element type was used in the current investigation. The grid points are not distributed uniformly over the computational domain as shown in figs. 2 and 3. They have greater intensity near the inner and outer surfaces of the cylinders in the radial direction. The spacing expansion and contraction factors were selected 10 and 0.1, respectively.

The numerical results are checked for grid independency. The numerical results are obtained with increasing number of nodes till further refinement in grid size. The effect of the mesh size on the solution is examined by solving sample cases of the current problem for different meshing systems. Table 1 indicates the effect of grid size on solution results. As shown in the left side of the table, the grid number in the angular direction is kept at

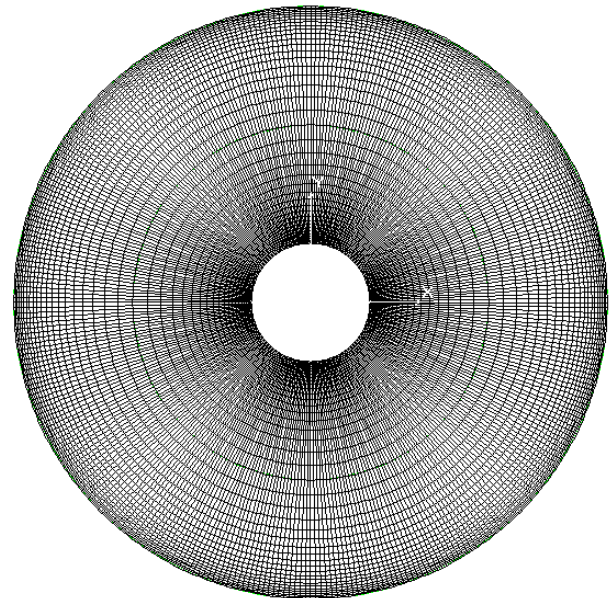


Fig. 2. Grid system.

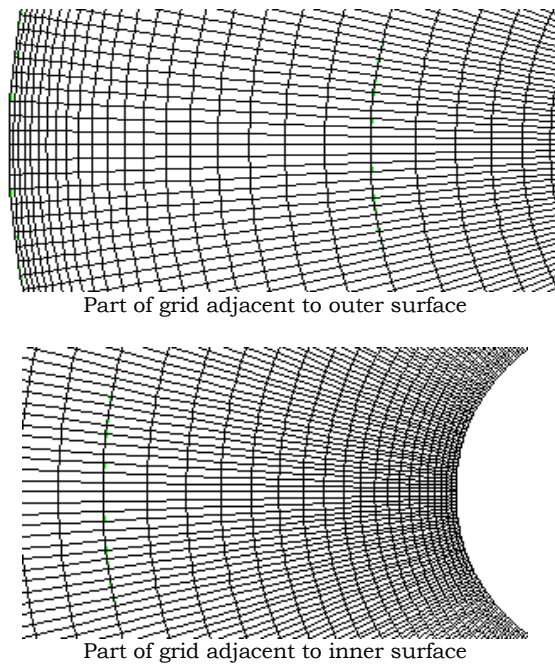


Fig. 3. Grid at outer and inner surfaces.

360, however, increasing grid number in radial direction from 20 to 30 reduces difference in total heat transfer from 2.18% to 0.45% from its value at grid number of 40×360. As indicated in the right side of the table, the grid number in radial direction is kept at 40. Increasing grid number in the angular direction, from 240 to 480, results in small difference in

the total heat transfer, 0.08 to -0.1%, from its value at grid number of 40×360. Upon the results of this investigation a grid system of 40×360 is chosen to be used in the following analysis.

4. Results and discussions

Table 2 shows the input data employed in the present investigation. Natural convection in enclosures of four D_o/D_i ratios was investigated. Typical samples of velocity vectors and stream function and iso-thermal lines are shown in figs. 4 to 6. The temperature and flow field results are in excellent qualitative agreement with the results of [3, 6, 7 and 17]. Two large eddies are set up in the buoyancy driven flow. Large velocity and temperature gradients exist in the vicinity of the hot and cold walls.

For low temperature differences (0.1-1 K), the plots of velocity vectors (as shown in fig. 4) show that the fluid circulates as a kidney-shaped pattern with a good agreement with the results of Bishop et al [4]. The circulation centers move up as the temperature difference increases. The fluid moves up near the inner hot surface and down near the outer cold surface. The velocity is very low near the

Table 1
Effect of grid size on solution results

$D_o = 0.06\text{m}$ $D_i = 0.03\text{m}$ $\Delta T = 40\text{ K}$	Effect of grid size in radial direction			Effect of grid size in angular direction		
	Meshing	$Q, \text{W/m}$	$\Delta Q/Q\%$	Meshing	$Q, \text{W/m}$	$\Delta Q/Q\%$
	20×360	20.112	2.18	40×240	19.698	0.08
	30×360	19.772	0.45	40×360	19.683	0
	40×360	19.683	0	40×480	19.662	-0.11

Table 2
Run conditions

D_o, m	D_i, m	D_o/D_i	T_i, K	T_o, K
0.06	0.03	2	300.01	300
0.06	0.02	3	to	
0.08	0.02	4	500	
0.1	0.02	5		

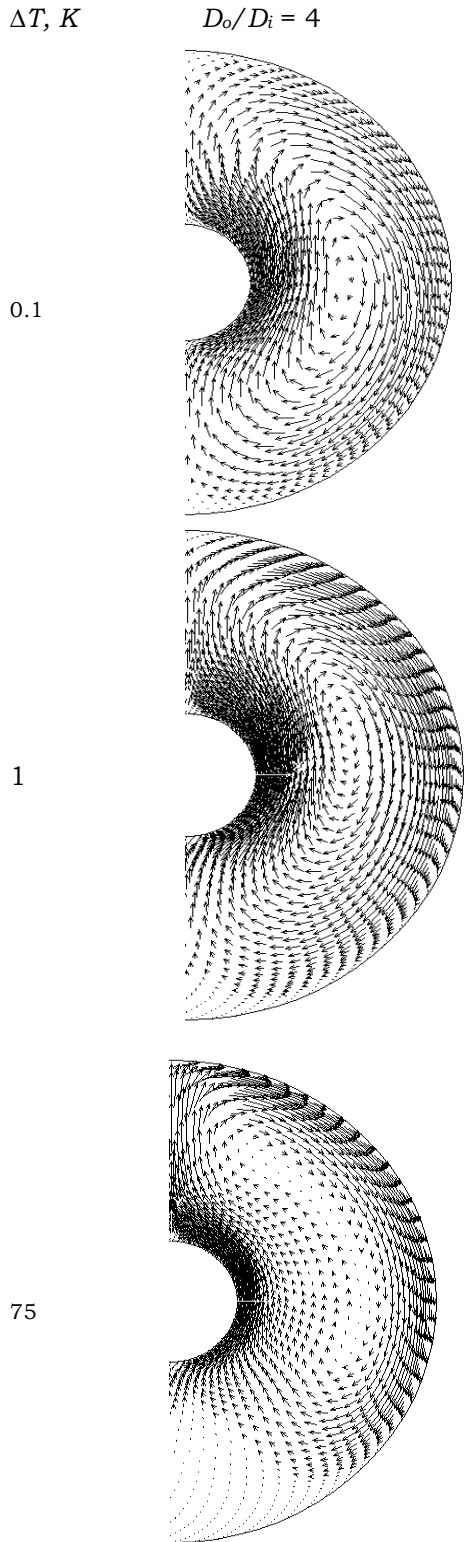


Fig. 4. Velocity vectors in annulus.

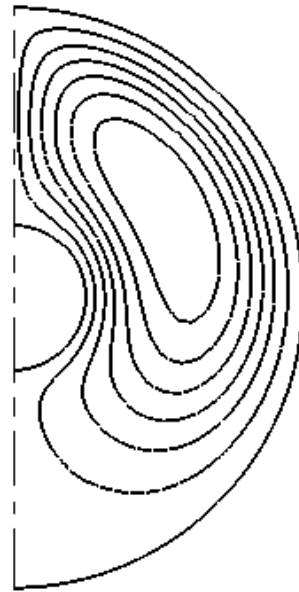


Fig. 5. Stream lines for $D_o/D_i = 4$ and $\Delta T = 10 K$.

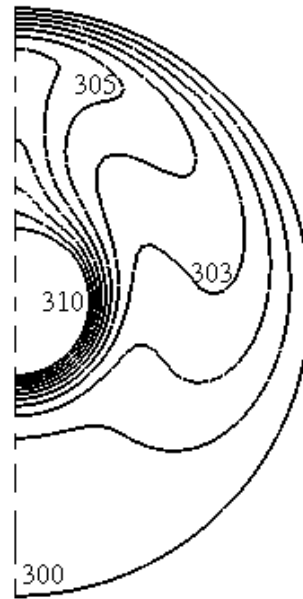


Fig. 6. Isothermal lines for $D_o/D_i = 4$ and $\Delta T = 10 K$.

circulation centers. Above 1 K temperature difference, the boundary layer along the inner and outer cylindrical surfaces can be observed and high velocity and temperature gradients exist near the inner hot and outer cold surfaces. As shown in the figures, the flow

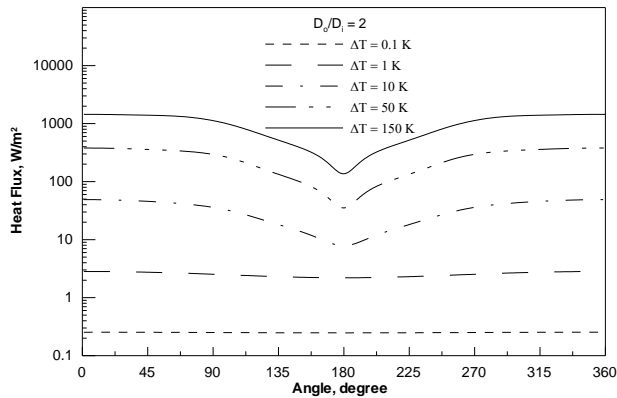


Fig. 7. Heat flux distributions along the inner surface for $D_o/D_i = 2$.

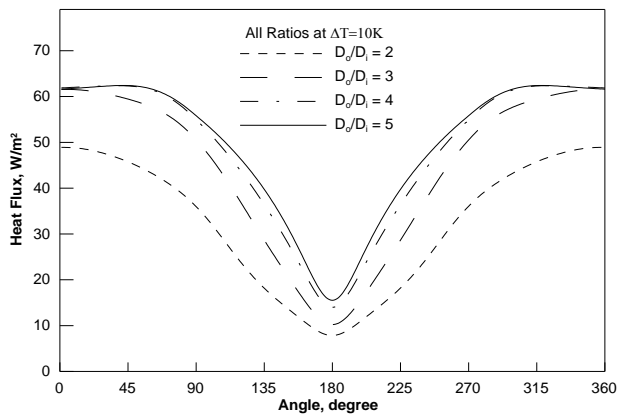


Fig. 8. Heat flux distributions along the inner surface for different diameter ratios at $\Delta T = 10$ K.

pattern intensifies as well as moves upward as the temperature difference increases.

The heat transfer from the inner to the outer wall was calculated by integrating the local heat flux along the inner wall,

$$Q = \int_{A_i} q_w dA, \quad (7)$$

where the local heat flux was estimated by applying Fourier's law at the surface of the inner cylinder,

$$q_w = -k \left. \frac{\partial T}{\partial n} \right|_w, \quad (8)$$

where n is the normal direction to the wall. Local heat flux distributions along the surface

of the inner cylinder are shown in figs. 7 and 8, where 0° and 360° angles represent the lower point of the inner cylinder and 180° angle represents the upper point of the inner cylinder. For low temperature difference, 0.1 K, the heat flux is uniform along the surface of the inner cylinder. These results indicate that the conduction heat transfer mechanism is the dominant. As shown in the figures, as the temperature difference increases, >1 K, the heat flux concentrates near the bottom of the inner cylinder, at 0° , due to small thickness of boundary layer at this point. The heat transfer decreases as we move up along the inner surface. The heat flux reaches its minimum value at upper point of cylinder surface at angle = 180° . These results indicate that the convection heat transfer mechanism is the dominant mechanism for larger values of temperature difference ($T > 1$).

Nusselt number based on the inner cylinder diameter was defined as,

$$Nu_i = \frac{h_i D_i}{k}, \quad (9)$$

where h_i is the average heat transfer coefficient along the inner wall and it is estimated as,

$$h_i = \frac{Q}{(T_i - T_o) A_i}. \quad (10)$$

The data of Nusselt number for the investigated conditions, listed in table 2, are shown in fig. 9. As shown in the figure, Nusselt number based on the inner cylinder diameter was represented versus Rayleigh number based on the inner cylinder diameter for the examined enclosure diameter ratios: 2, 3, 4 and 5. As shown in the figure, Nusselt number increases as Rayleigh number increases for a given diameter ratio. The results indicate that there are three distinct regimes of heat transfer. The first is the conduction dominated regime where the Nusselt number is approximately constant. The data in this region were obtained by reducing the temperature difference between the inner and outer cylinders from 0.1 to 0.01 K. For $D_o/D_i = 2.0$, the conduction dominated regime falls in the region where Ra_i

< 2000. The third regime of heat transfer is the convection dominated regime where $Ra_i > 11000$. The trend of the data in this region shows strong dependency on Rayleigh number Ra_i . The region between the above Ra_i values is the second regime which is a transition region between the conduction and convection.

The effect of the diameter ratio D_o/D_i on Nusselt number data is also shown in fig. 9. For low Rayleigh number, i.e. the conduction dominated regime, the Nusselt number is higher for low diameter ratio. This is true since the dominated mechanism is the conduction heat transfer mechanism in which the heat transfer increases as annular thickness, or D_o/D_i decreases. For high Rayleigh number, i.e. the convection dominated regime, the heat transfer represented by Nusselt number increases as the diameter ratio increases. In this region where the convection mechanism is the dominant heat transfer mechanism, increasing the annulus gap gives the opportunity to the boundary layer and plume to develop as shown in fig. 6.

The pure conduction limits for heat transfer in cylindrical annuli were obtained by solving the problem as a pure conduction problem. The conduction limit for the annulus can be obtained from conduction analysis through the cylindrical air film. The heat transfer by conduction per unit length through the annular gap is:

$$Q_{cond} = \frac{2 \pi k (T_i - T_o)}{\ln(D_o / D_i)} \tag{11}$$

This equation can be rearranged to give Nusselt number which represents the conduction dominated region,

$$Nu_{icond} = \frac{2}{\ln(D_o / D_i)} \tag{12}$$

another method to represent heat transfer data in the annulus is to represent it in terms of the effective thermal conductivity ratio k_e/k , where k_e is an equivalent thermal conductivity for both of conduction and convection in the annulus. The equivalent thermal conductivity k_e can be estimated from:

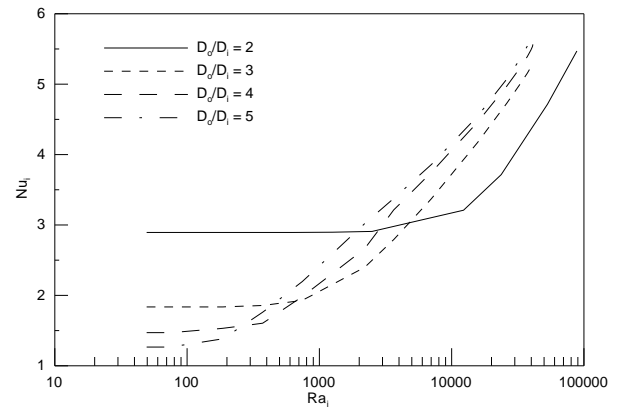


Fig. 9. Nusselt number versus Rayleigh number for different annulus diameter ratios.

$$Q = \frac{2 \pi k_e (T_i - T_o)}{\ln(D_o / D_i)} \tag{13}$$

The data of the effective thermal conductivity ratio k_e/k for the conditions listed in table 2 are shown in fig. 10. As shown in the figure, this ratio is represented versus Rayleigh number based on the inner cylinder diameter for the examined enclosure diameter ratios: 2, 3, 4 and 5. The pure conduction heat transfer limit is one. As shown in the figure, there are three distinct regimes of heat transfer. The first regime is the conduction dominated regime where the effective thermal conductivity ratio $k_e/k = 1$. The third is the convection dominated regime where the curve shows strong dependency on Rayleigh number. The second regime which falls between the above mentioned regimes is a transition regime.

These data are regrouped as shown in Fig.11 by changing the horizontal axis to a modified Rayleigh number Ra_m , where Ra_m is:

$$Ra_m = Ra_i^{1/4} \left[0.1389 \left(1 - \frac{D_i}{D_o} \right) + 0.0927 \right] \ln \left(\frac{D_o}{D_i} \right) \tag{14}$$

The symbols in the figure represent the current numerical data while the solid line represents the best fitting of the current data.

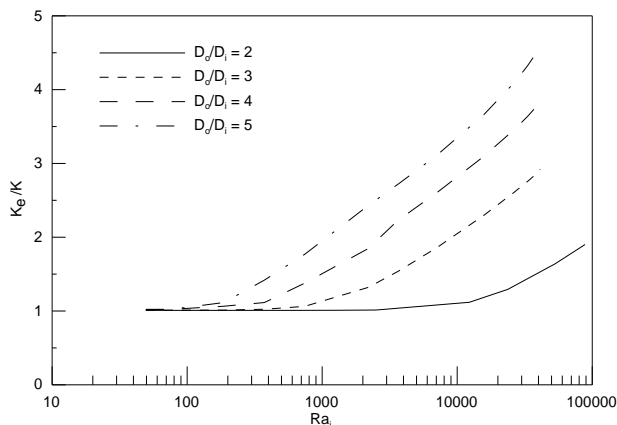


Fig. 10. Thermal conductivity ratio versus Rayleigh number.

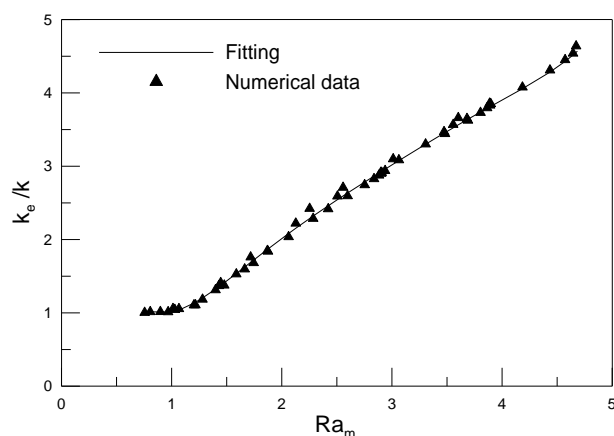


Fig. 11. Thermal conductivity ratio versus modified Rayleigh number.

$$\frac{k_e}{k} = 0.0123Ra_m^6 - 0.2167Ra_m^5 + 1.5514Ra_m^4 - 5.7568Ra_m^3 + 11.553Ra_m^2 - 10.683Ra + 4.5486. \quad (15)$$

Three regions can be distinguished in fig. 11. Conduction dominated regime, $Ra_m < 0.8$, where $k_e/k = 1$, convection dominated regime, $Ra_m > 1.5$ and a transition regime between them.

The current numerical technique is validated by comparing the current numerical data with data from literature. Fig. 12 shows the comparison between current data and experimental data of Grigull and Hauf [2]. As shown in the figure, the best fitting of the cur-

rent numerical data, represented by the solid line, represents accurately the experimental data of [2] for various diameter ratios. As shown in the figure, most of the data fall within -5% to +10% of the prediction of current model. As shown in fig. 13, the current model represents accurately the experimental data of [6] for various diameter ratios.

Fig. 14 shows the comparison between current model and correlations available in the literature. First, the comparison indicates the significant differences between available models. As shown in the figure, the correlations of Liu et al. [1] and Kraussold as given in [17] underpredict the current numerical data while the correlations of Kuehn and Goldstein [7] and Grigull and Hauf [2] overpredict the current data. The predictions of the correlations of Lis [3] and Raithby and Hollands [8] are close to the current numerical data.

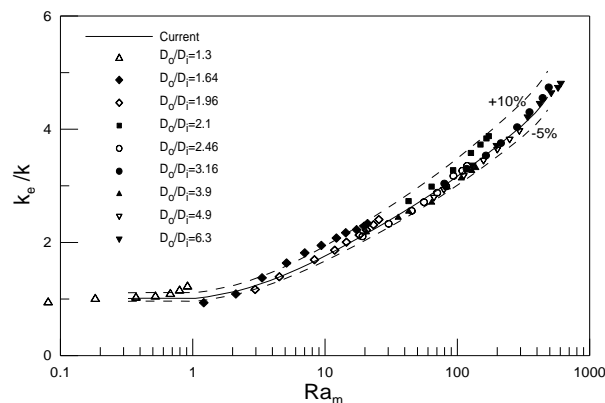


Fig. 12. Comparison between current data and experimental data of Grigull and Hauf [2].

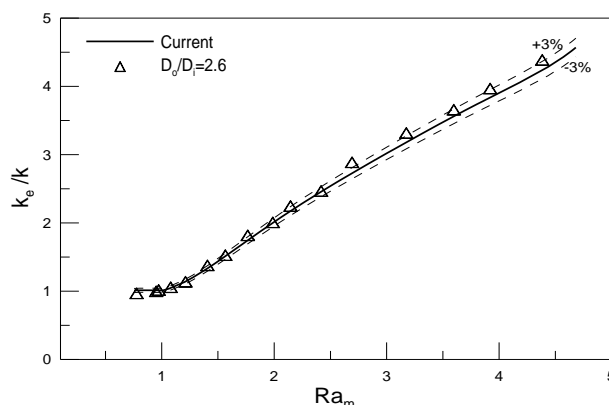


Fig. 13. Comparison between current data and experimental data of Kuehn and Goldstein [6].

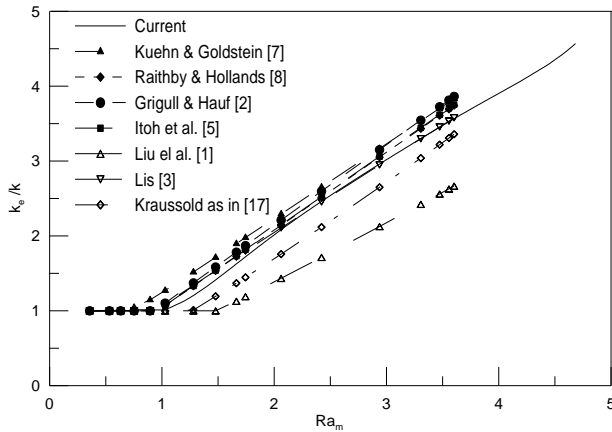


Fig.14. Comparison between current data and available correlations.

5. Conclusions

Natural convection heat transfer in air between two horizontal concentric cylinders was investigated numerically using finite element technique. Laminar conditions up to Rayleigh number Ra_i of 10^5 were investigated. Effects of annulus diameter ratio and Rayleigh number on this type of flow were investigated. The data were represented in terms of Nusselt number Nu_i and the effective thermal conductivity ratio k_e/k versus Rayleigh number Ra_i . As introduced by [2] three regimes of heat transfer were obtained; dominated conduction, transition and dominated convection regimes. The effective thermal conductivity ratio $k_e/k = 1$ in the first regime. The numerical data for diameter ratios of $D_o/D_i = 2$ to 5 were grouped by representing effective thermal conductivity ratio k_e/k versus a new modified Rayleigh number Ra_m , eq. (14). A new correlation for effective thermal conductivity ratio k_e/k was introduced. The current correlation is compared with experimental data available in the literature. The comparison shows a very good agreement between current results and the experimental data of Grigull and Hauf [2] and Kuehn and Goldstein [6].

Nomenclature

A_i is the surface area of inner cylinder, m^2
 C_p is the specific heat, J/kg K,
 D_i is the diameter of the inner cylinder, m
 D_o is the diameter of the outer cylinder, m

Gr_δ is the grashof number based on gap thickness, $g \beta(T_o-T_i) \delta^3 / \nu^2$,
 Gr_i is the grashof number based on inner cylinder diameter, $g \beta(T_o-T_i) D_i^3 / \nu^2$,
 g is the gravity acceleration, m/s^2
 h_i is the average heat transfer coefficient along the inner cylinder, $W/m^2 K$
 k is the thermal conductivity of fluid, $W/m K$,
 k_e is the effective thermal conductivity, $W/m K$,
 Nu_i is the nusselt number based on inner cylinder diameter, $h_i D_i / k$,
 $Nu_{i,cond}$ is the nusselt number for pure conduction, $h_{i,cond} D_i / k$,
 P is the pressure, Pa,
 Pr is the Prandtl number,
 T is the temperature, K,
 T_i is the temperature of inner cylinder, K,
 T_o is the temperature of outer cylinder, K,
 T_m is the mean temperature, K,
 Ra_i is the Rayleigh Number based on inner cylinder diameter, $Gr_i Pr$,
 Ra_m is the modified Rayleigh Number eq. (14),
 Q is the heat transfer, W,
 Q_{cond} is the conductive heat transfer, W,
 q_w is the local heat flux, W/m^2 ,
 u is the velocity in x direction, m/s,
 v is the velocity in y direction, m/s,
 x is the horizontal coordinate, m,
 y is the vertical coordinate, m,

Greek symbols

β is the Volumetric thermal expansion coefficient, K^{-1}
 δ is the enclosure gap $[(D_o - D_i) / 2]$, m
 ν is the kinematic viscosity, m^2/s
 μ is the dynamic viscosity, Pa s
 ρ is the fluid density, kg/m^3

Subscripts

cond is the conduction,
conv is the convection,
i is the inner cylinder, and
o is the outer cylinder.

References

[1] C. Liu, W.K. Mueller and F. Landis, "Natural Convection Heat Transfer in

- Long Horizontal Cylindrical Annuli", ASME International Developments in Heat Transfer, Paper #117, pp. 976-984 (1961).
- [2] U. Grigull and W. Hauf, "Natural Convection in Horizontal Cylindrical Annuli" Proceeding of the 3rd International Heat Transfer Conference, Vol. 2, pp. 182-195 (1966).
- [3] C. Lis, "Experimental Investigation of Natural Convection Heat Transfer in Simple and Obstructed Horizontal Annuli", Proceeding of the 3rd International Heat Transfer Conference, Vol. 2, pp. 196-204 (1966).
- [4] E.H. Bishop, C.T. Carley and R.E. Powe, "Natural Convection Oscillatory Flow in Cylindrical Annuli", Int. J. Heat Mass Transfer, Vol. 11, pp. 1741-1752 (1968).
- [5] M. Itho, T. Fujita, N. Nishiwaki and M. Hirata, "A New Method of Correlating Heat Transfer Coefficients for Natural Convection in Horizontal Cylindrical Annuli," International Journal of Heat and Mass Transfer, Vol. 13, pp.1364-1368 (1970).
- [6] T.H. Kuehn and R.J. Goldstein, "An Experimental and Theoretical Study of Natural Convection in the Annulus between Horizontal Concentric Cylinders", J. Fluid Mechanics, Vol. 74 (4), pp. 695-719 (1974).
- [7] T.H. Kuehn and R.J. Goldstein, "Correlating Equations for Natural Convection Heat Transfer Between Horizontal Circular Cylinders", Int. J. Heat Mass Transfer, Vol. 19, pp. 1127-1134 (1976).
- [8] G. Raithby and K. Hollands, "A General Method of Obtaining Approximate Solutions to Laminar and Turbulent Free Convection Problem," Advances in Heat Transfer, eds. T.F. Irvine Jr. and J.P. Hartnett, Academic Press, New York, pp. 265-315 (1975).
- [9] R. Kumar, "Study of Natural Convection in Horizontal Annuli", Int. J. Heat Mass Transfer, Vol. 31 (6), pp. 1137-1148 (1988).
- [10] J.S. Yoo, "Natural Convection in a Narrow Horizontal Cylinder Annulus: Pr ≤ 0.3", Int. J. Heat Mass Transfer, Vol. 41, pp. 3055-3073 (1998).
- [11] J.S. Yoo, "Prandtl Number Effect on Bifurcation and Dual Solution in Natural Convection in Horizontal Annulus", Int. J. Heat Mass Transfer, Vol. 42, pp. 3279-3290 (1999).
- [12] L. Crawford and R. Lemlich, "Natural Convection in Horizontal Concentric Cylindrical Annuli", Industrial and Engineering Chemistry Fundamentals, Vol. 1 (1), pp. 260-264 (1962).
- [13] B. Farouk and S.I. Güçeri, "Laminar and Turbulent Natural Convection in the Annulus between Horizontal Concentric Cylinders", J. Heat Transfer, Vol. 104, pp. 631-636 (1982).
- [14] P.M. Kolesnikov, and V.I. Bubnovich, "Non-Stationary Conjugate Free-Convection Heat Transfer in Horizontal Cylindrical Coaxial Channels", Int. J. Heat Mass Transfer, Vol. 31 (6), pp. 1149-1155 (1988).
- [15] C. Kim, and T. Ro, "Numerical Investigation on Bifurcative Natural Convection in an Air-Filled Horizontal Annulus", J. Heat Transfer, Vol. 116, pp. 135-141 (1994).
- [16] S.M. ElSherbiny, and A.R. Moussa, "Natural Convection in Air Layers between Horizontal Concentric Isothermal Cylinders", Alexandria Engineering Journal, Vol. 43, pp. 297-311 (2004).
- [17] P. Teertstra and M.M. Yovanovich, "Comprehensive Review of Natural Convection in Horizontal Annuli", 7th AIAA/ASME Joint Thermophysics and Heat Transfer Conference, Albuquerque, NM, June15-18, HTD- Vol. 357-4, pp. 141-152 (1998).
- [18] S.V. Patankar, 1980, Numerical Heat Transfer and Fluid Flow, McGraw Hill.
- [19] Zeitoun, O., "Natural Convection from a Vertical Plate in a Horizontal Cylinder", Int. J. of heat and Technology, Vol. 23 (1) (2005).
- [20] O. Zeitoun and M. Ali, "Natural Convection Heat Transfer from Isothermal Horizontal Rectangular Ducts", Submitted for Publication in Alexandria Engineering Journal (2005).

Received August 6, 2005
Accepted September 23, 2005

